COMMUNICATIONS

Photolysis of ICl causes mass-dependent interference in the Cl($^2P_{3/2}$) photofragment angular momentum distributions

T. Peter Rakitzis, S. Alex Kandel, and Richard N. Zare
Department of Chemistry, Stanford University, Stanford, California 94305

(Received 20 February 1998; accepted 18 March 1998)

We have studied the photodissociation of ICl using linearly polarized light at 532 nm. This wavelength excites several electronic states. Using linearly polarized probe light, we have measured the angular momentum distributions of the ^{35}Cl($^2P_{3/2}$) and ^{37}Cl($^2P_{3/2}$) photofragments, which are found to differ significantly. These distributions are expressed in a multipole moment expansion having four terms. These terms can be classified as incoherent contributions from parallel and perpendicular transitions, and coherent contributions from interference that arises from these interacting states. Analysis of these angular momentum distributions using this formalism shows that the incoherent contributions from the dissociating surfaces are mass independent, whereas the coherent contributions are mass dependent. © *1998 American Institute of Physics.* [S0021-9606(98)03720-9]

As predicted by van Brunt and Zare,[1] photodissociation of a diatomic molecule can produce atomic photofragments with a highly anisotropic angular momentum distribution. A recent experimental study by Eppink *et al.*[2] reported the observation of maximally aligned O($^1D_2$) atoms from the photolysis of O_2 in the $b\ ^1\Sigma_g^+$ state. In their study, the angular momentum, **j**, of the O($^1D_2$) photofragment is found to occupy almost exclusively the $m_j=0$ state, so that **j** always points perpendicular to the recoil direction. The production of these maximally aligned O($^1D_2$) atoms depends on the fact that the photoexcitation is well-defined (the transition is pure parallel in character), and that the subsequent dissociation process is rapid (axial recoil) and adiabatic. This behavior is often the case but the presence of multiple dissociative states and nonadiabatic effects can produce much more complicated photofragment angular momentum distributions. An example of this more complex dissociation dynamics is reported in this Communication.

In this work we photolyze ICl with linearly polarized light at 532 nm, and we probe the Cl($^2P_{3/2}$)photofragments with linearly polarized light at 235 nm using (2+1) resonance-enhanced multiphoton ionization (REMPI). The recorded signal is sensitive to the angular momentum distribution of the Cl($^2P_{3/2}$) photofragments. This distribution can be described by a multipole moment expansion, as shown in the full quantum mechanical treatment of Siebbeles *et al.*[3] We modify the previous treatment by Siebbeles *et al.* and introduce the polarization parameters $\mathbf{a_q^{(k)}}(\parallel)$, $\mathbf{a_q^{(k)}}(\perp)$, and $\mathbf{a_q^{(k)}}(\parallel,\perp)$ to describe the photofragment angular momentum distribution in the molecular frame.[4] These parameters are related to the well-known polarization parameters, $\mathbf{A_q^{(k)}}$.[5,6] The parameters $\mathbf{a_q^{(k)}}(\parallel)$ describe the contributions to the photofragment angular momentum distribution that arises solely from dissociative surfaces accessed through parallel transitions, the $\mathbf{a_q^{(k)}}(\perp)$ describe the contributions that arise solely from dissociative surfaces accessed through perpendicular transitions, whereas the $\mathbf{a_q^{(k)}}(\parallel,\perp)$ describe the contributions that arise solely from the interference between the parallel and perpendicular dissociative surfaces. The total angular momentum of the photofragment, $j=3/2$, restricts k to be less than 4; the use of linearly polarized probe light restricts experimental sensitivity to parameters with even k. Consequently, the experiments reported here are sensitive to only four parameters $\mathbf{a_0^{(2)}}(\parallel)$, $\mathbf{a_0^{(2)}}(\perp)$, $\mathrm{Re}[\mathbf{a_1^{(2)}}(\parallel,\perp)]$, and $\mathbf{a_2^{(2)}}(\perp)$, which are all real. The relative ionization probability of a photofragment in terms of these polarization parameters and the orientation of the recoil direction with respect to the photolysis and probe laser polarization directions is given by

$$I(\Theta,\Phi,\theta_\epsilon,\beta,\mathbf{a_q^{(k)}}) = 1 + s_2 G_c^2[(1+\beta)\cos^2\theta_\epsilon P_2(\cos\Theta)\mathbf{a_0^{(2)}}(\parallel) + (1-\beta/2)\sin^2\theta_\epsilon P_2(\cos\Theta)\mathbf{a_0^{(2)}}(\perp)$$
$$+ \sqrt{3/2}\sqrt{(1+\beta)(1-\beta/2)}\,\sin 2\theta_\epsilon \sin 2\Theta \cos\Phi\ \mathrm{Re}[\mathbf{a_1^{(2)}}(\parallel,\perp)]$$
$$+ \sqrt{3/2}(1-\beta/2)\sin^2\theta_\epsilon \sin^2\Theta \cos 2\Phi\, \mathbf{a_2^{(2)}}(\perp)]/[1+\beta P_2(\cos\theta_\epsilon)], \quad (1)$$

where β is the photofragment spatial anisotropy, θ_ϵ is the angle between the recoil direction and the photolysis laser polarization, Θ is the angle between the recoil direction and the probe laser polarization, Φ is the azimuthal angle of the photolysis and probe polarizations about the recoil direction, G_c^2 is the long-time-limit hyperfine depolarization coefficient[7] which, in this study, is equal to 0.27, and s_2 is the relative sensitivity of the parameters with $k=2$,[8] and is equal to $-5/4$ in this study. The form of Eq. (1) will be justified in a later publication.[4] Equation (1) is used in the fitting of the measured polarization-dependent time-of-flight profiles to obtain the polarization parameters. The angular momentum distribution, D, in the molecular frame is then given by

$$D(\theta,\varphi,\theta_\epsilon,\beta,\mathbf{a}_\mathbf{q}^{(\mathbf{k})}) = 1+[(1+\beta)\cos^2\theta_\epsilon P_2(\cos\theta)\mathbf{a}_\mathbf{0}^{(2)}(\|)+(1-\beta/2)\sin^2\theta_\epsilon P_2(\cos\theta)\mathbf{a}_\mathbf{0}^{(2)}(\perp)$$
$$+\sqrt{3/2}\sqrt{(1+\beta)(1-\beta/2)}\sin 2\theta_\epsilon \sin 2\theta\cos\varphi\ \mathrm{Re}[\mathbf{a}_\mathbf{1}^{(2)}(\|,\perp)]$$
$$+\sqrt{3/2}(1-\beta/2)\sin^2\theta_\epsilon\sin^2\theta\cos 2\varphi\mathbf{a}_\mathbf{2}^{(2)}(\perp)]/[1+\beta P_2(\cos\theta_\epsilon)], \quad (2)$$

where θ and φ are the spherical polar angles.

The experimental apparatus and techniques have been described elsewhere.[9,10] Briefly, liquid ICl and 800 Torr of helium gas are mixed in a bulb cooled in an ice bath; the resulting gas mixture is then expanded through a pulsed nozzle into the vacuum chamber with a backing pressure of 380 Torr. The ICl is photolyzed with linearly polarized 532 nm light (100 mJ/pulse) from the frequency-doubled output of a Nd^{3+}:YAG laser, which is gently focused into the detection region. After 20 ns, the Cl ($^2P_{3/2}$) atom photofragments are detected via (2+1) REMPI through the $3p^4\ 4p\ ^2S_{1/2}$ level. The linearly polarized 235 nm probe light (100 μJ/pulse) is generated from the frequency-doubled output of a Nd^{3+}:YAG-pumped tunable dye laser, and it intersects the ionization region at the focus of a 1.1 m lens. The $^{35}Cl^+$ and $^{37}Cl^+$ ions are detected with a Wiley–McLaren time-of-flight mass spectrometer operated under velocity-sensitive conditions; the voltage conditions are chosen to ensure that the ion-packet radius is always smaller than the microchannel-plate radii, such that all ions are detected. $I^{35}Cl$ and $I^{37}Cl$ are present in their natural abundance of approximately 3:1. The Cl-atom speed distribution is measured to be monoenergetic, showing that we are observing only a one-photon photolysis of ICl.

Figure 1 presents the probe-differenced time-of-flight profiles for the $^{35}Cl^+$ and $^{37}Cl^+$ ions. These profiles are the difference of profiles in which the probe polarization is parallel and perpendicular to the time-of-flight axis. This subtraction procedure is accurate to better than 1% of the total signal, whereas the difference signals are greater than 10% of the total signal. Additionally, these difference profiles are proportional to the polarization parameters. The two photolysis polarization geometries are the minimum required to measure all four polarization parameters.

The fit of the profiles shown in Fig. 1 yields the $\mathbf{a}_\mathbf{0}^{(2)}(\|)$, $\mathbf{a}_\mathbf{0}^{(2)}(\perp)$, $\mathrm{Re}[\mathbf{a}_\mathbf{1}^{(2)}(\|,\perp)]$, and $\mathbf{a}_\mathbf{2}^{(2)}(\perp)$, for both ^{35}Cl and ^{37}Cl, and the results are presented in Fig. 2. The fit yields a startling result: the incoherent contributions to the polarization, the $\mathbf{a}_\mathbf{0}^{(2)}(\|)$, $\mathbf{a}_\mathbf{0}^{(2)}(\perp)$, and $\mathbf{a}_\mathbf{2}^{(2)}(\perp)$ are identical, within error, for both ^{35}Cl and ^{37}Cl; in contrast, the coherent contribution to the polarization, the $\mathrm{Re}[\mathbf{a}_\mathbf{1}^{(2)}(\|,\perp)]$ parameter, is strongly positive for ^{35}Cl but strongly negative for ^{37}Cl. Apparently, it is this coherent parameter that is entirely responsible for the differences observed in the angular momentum distributions of the ^{35}Cl and ^{37}Cl photofragments. This polarization parameter analysis isolates the coherent and incoherent contributions from parallel and perpendicular transitions. Therefore, we believe this formalism is both natural and physical for describing photofragment angular distributions. The molecular frame parameters used here will be discussed extensively in a future publication.[4]

The measured molecular frame parameters, with the use of Eq. (2), can be used to depict the molecular frame angular momentum distribution. In Fig. 3, we show the dependence

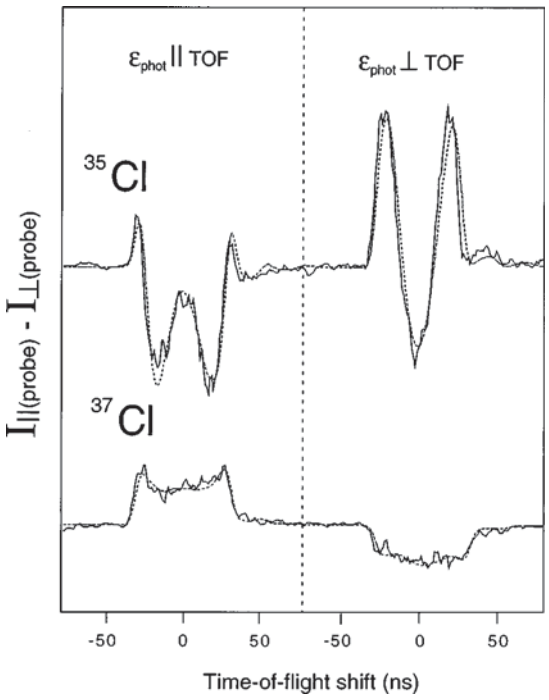

FIG. 1. Probe-differenced time-of-flight profiles with the photolysis polarization parallel and perpendicular to the time-of-flight axis, for both ^{35}Cl and ^{37}Cl photofragments. These profiles are proportional to the polarization parameters that describe the photofragment angular momentum distributions. Notice how different the signals are for the ^{35}Cl and ^{37}Cl photofragments. The dashed lines are the fits to the data of basis functions generated with Eq. (1) from which the polarization parameters are determined.

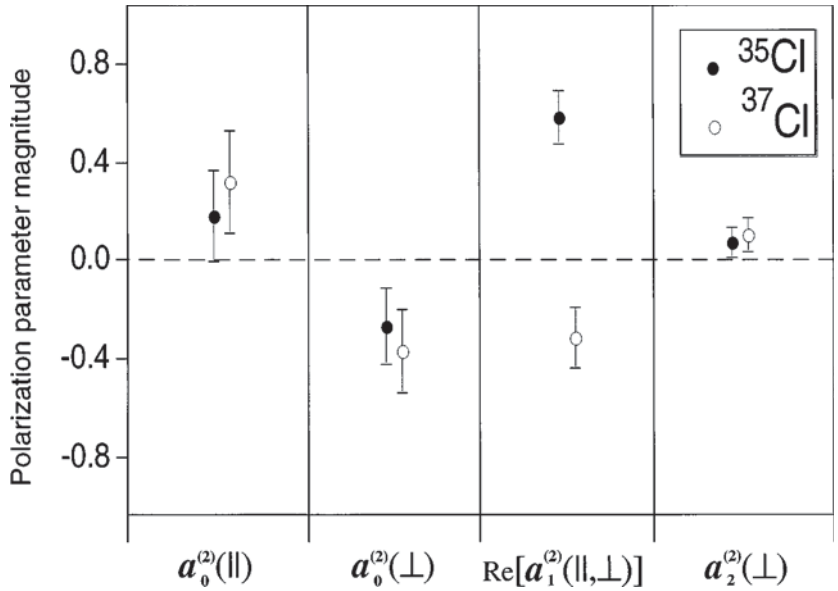

FIG. 2. The polarization parameters resulting from the fits shown in Fig. 1. The incoherent parameters, $\mathbf{a}_0^{(2)}(\|)$, $\mathbf{a}_0^{(2)}(\perp)$, and $\mathbf{a}_2^{(2)}(\perp)$ are identical, within error, for the ^{35}Cl and ^{37}Cl photofragments, whereas the coherent parameter, the $\mathrm{Re}[\mathbf{a}_1^{(2)}(\|,\perp)]$, differs markedly for the ^{35}Cl and ^{37}Cl photofragments.

of the alignment of the angular momentum of the ^{35}Cl and ^{37}Cl photofragments as a function of the direction the photolysis polarization makes with respect to the photofragment recoil velocity, **v**. When the photolysis polarization is parallel or perpendicular to the recoil direction, the excitation light accesses pure parallel or perpendicular transitions, and the angular momentum distributions depend on the incoherent polarization parameters only. As can be seen in Fig. 2, the incoherent polarization parameters for the ^{35}Cl and ^{37}Cl photofragments are identical within error. Consequently, we expect that the photofragments should possess the same angular momentum distributions. Figure 3 shows that, in these cases, the ^{35}Cl and ^{37}Cl photofragments possess very similar angular momentum distributions; the small differences indicate the uncertainties in the measurements. In contrast, when the photolysis polarization is at an intermediate angle, Fig. 3 shows that the angular momentum distributions peak at intermediate angles, but with an opposite sense for ^{35}Cl and ^{37}Cl. This effect, which breaks planar symmetry (defined by **v** and $\mathbf{v}\times\boldsymbol{\epsilon}_{\mathrm{phot}}$), can only arise from interference effects.

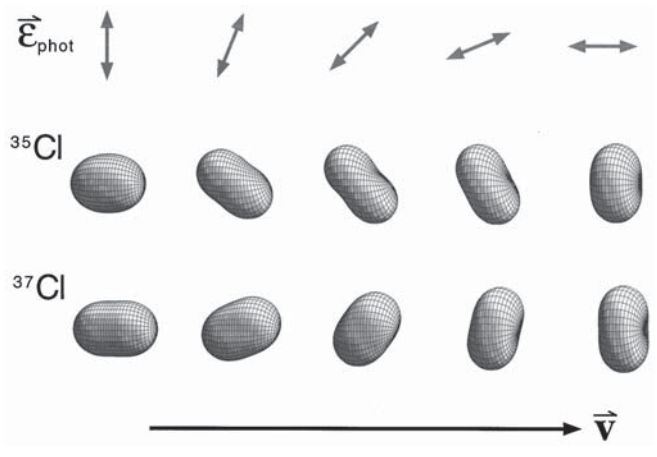

FIG. 3. The molecular frame alignment of the ^{35}Cl and ^{37}Cl photofragment angular momentum distributions as a function of the direction the photolysis polarization makes with respect to the recoil direction (in equal steps of 22.5°). Notice how the ^{35}Cl and ^{37}Cl angular momentum distributions are nearly identical when the photolysis polarization is parallel ($\theta_\epsilon = 0°$) or perpendicular ($\theta_\epsilon = 90°$) to the recoil direction, **v**, whereas the distributions are very different when the photolysis polarization is at an intermediate angle, θ_ϵ.

The photofragment spatial distribution is measured to be approximately isotropic for both the ^{35}Cl and ^{37}Cl photofragments, i.e., the β parameter for both photofragments is near zero. This measurement indicates that 532 nm light accesses excited states that are of both parallel and perpendicular character. We believe that these states are $^3\Pi_{0+}$ and $^1\Pi_1$.[11,12] In these experiments, no information can be obtained from the spatial anisotropy about the nature of the coherence of this excitation process. Photofragment vector correlations have long been considered a useful probe of photodissociation dynamics.[13,14] We have observed that Cl ($^2P_{3/2}$) atoms from ICl photolysis are strongly aligned. Furthermore, the alignment parameter measurements show coherences between parallel and perpendicular excited states. It is particularly interesting that the coherences for ^{35}Cl and ^{37}Cl are markedly different, especially as there are no isotope effects in the excitation cross section, spatial anisotropy, or incoherent alignment parameters. Several of the excited states of ICl are bound and support vibrational structure; therefore, it is possible that vibronic effects could influence the photodissociation dynamics in a mass-dependent fashion. Additionally, we have measured that the polarization parameters do not depend on whether photolysis laser is injection-seeded; thus, we conclude that the interference effects are not sensitive to 1 cm^{-1} variations of the photolysis energy, and thus are not the result of a sharp resonance. Work is in progress in our laboratory measuring the orientation of the Cl atoms using circularly polarized probe light and investigating how the photodissociation dynamics change with excitation energy. The results presented in this Communication demon-

strate that the measurement and characterization of the photofragment angular momentum distribution can provide new insight into the nature of photodissociation dynamics.

This work has been supported by the National Science Foundation under Grant No. CHE-93-22690.

[1] R. J. van Brunt and R. N. Zare, J. Chem. Phys. **48**, 4304 (1968).
[2] A. T. J. B. Eppink, D. H. Parker, M. H. M. Janssen, B. Buijsse, and W. J. van der Zande, J. Chem. Phys. **108**, 1305 (1998).
[3] L. D. A. Siebbeles, M. Glass-Maujean, O. S. Vayutinskii, J. A. Beswick, and O. Roncero, J. Chem. Phys. **100**, 3610 (1994).
[4] T. P. Rakitzis and R. N. Zare (in preparation).
[5] R. N. Zare, *Angular Momentum, Understanding Spatial Aspects in Chemistry and Physics* (Wiley–Interscience, New York, 1988).
[6] A. J. Orr-Ewing and R. N. Zare, Annu. Rev. Phys. Chem. **45**, 315 (1994).
[7] A. J. Orr-Ewing, W. R. Simpson, T. P. Rakitzis, and R. N. Zare, Isr. J. Chem. **34**, 95 (1994).
[8] T. P. Rakitzis, S. A. Kandel, and R. N. Zare, J. Chem. Phys. **107**, 9382 (1997).
[9] W. R. Simpson, A. J. Orr-Ewing, S. A. Kandel, T. P. Rakitzis, and R. N. Zare, J. Chem. Phys. **103**, 7299 (1995).
[10] T. P. Rakitzis, S. A. Kandel, T. Lev-On, and R. N. Zare, J. Chem. Phys. **107**, 9392 (1997).
[11] K. Tonokura, Y. Matsumi, M. Kawasaki, L. K. Hong, S. Yabushita, S. Fujimora, and K. Saito, J. Chem. Phys. **99**, 3461 (1993).
[12] S. Yabushita (private communication).
[13] G. E. Hall, N. Sivakumar, P. L. Houston, and I. Burak, Phys. Rev. Lett. **56**, 1671 (1986).
[14] R. N. Dixon, J. Chem. Phys. **85**, 1866 (1986).